Endobronchial optical coherence tomography or computed tomography for evaluating progression of bronchiectasis

Lin-ling Cheng[1,4], Wei-jie Guan[1,2,4], Chang-hao Zhong[1], Chong-yang Duan[3], Zhu-quan Su[1], Shi-yue Li[1,5] and Nan-shan Zhong[1,5]

[1]State Key Laboratory of Respiratory Disease, National Clinical Research Center for Respiratory Disease, Guangzhou Institute of Respiratory Health, The First Affiliated Hospital of Guangzhou Medical University, Guangzhou Medical University, Guangzhou, China. [2]Department of Thoracic Surgery, Guangzhou Institute of Respiratory Disease, The First Affiliated Hospital of Guangzhou Medical University, Guangzhou, China. [3]State Key Laboratory of Organ Failure Research, National Clinical Research Center for Kidney Disease, Department of Biostatistics, School of Public Health, Southern Medical University, Guangzhou, China. [4]Joint first authors. [5]Joint senior authors.

Corresponding author: Nan-shan Zhong (nanshan@vip.163.com)

Shareable abstract (@ERSpublications)
Endobronchial optical coherence tomography imaging could reveal the evolution of thickened-walled bronchioles surrounding the dilated bronchi, indicating radiological progression of bronchiectasis https://bit.ly/3nJmQAV

Cite this article as: Cheng L-L, Guan W-J, Zhong C-H. Endobronchial optical coherence tomography or computed tomography for evaluating progression of bronchiectasis. *ERJ Open Res* 2023; 9: 00490-2022 [DOI: 10.1183/23120541.00490-2022].

Received: 7 Oct 2022
Accepted: 30 April 2023

Abstract

Background The early radiological signs of progression in bronchiectasis remain unclear. The objective of the present study was to compare endobronchial optical coherence tomography (EB-OCT) and chest computed tomography (CT) for the evaluation of radiological progression of bronchiectasis *via* stratification of the presence (TW^+) or absence (TW^-) of thickened-walled bronchioles surrounding dilated bronchi in patients with bronchiectasis based on CT, and determine the risk factors.

Methods In this prospective cohort study, we performed both chest CT and EB-OCT at baseline and 5-year follow-up, to compare changes in airway calibre metrics. We evaluated bacterial microbiology, sputum matrix metalloproteinase-9 levels and free neutrophil elastase activity at baseline. We compared clinical characteristics and airway calibre metrics between the TW^+ and TW^- groups. We ascertained radiological progression at 5 years *via* CT and EB-OCT.

Results We recruited 75 patients between 2014 and 2017. At baseline, EB-OCT metrics (mean luminal diameter (p=0.017), inner airway area (p=0.005) and airway wall area (p=0.009) of seventh- to ninth-generation bronchioles) were significantly greater in the TW^+ group than in the TW^-group. Meanwhile, EB-OCT did not reveal bronchiole dilatation (compared with the same segment of normal bronchioles) surrounding nondilated bronchi on CT in the TW^- group. At 5 years, 53.1% of patients in the TW^+ group progressed to have bronchiectasis measured with EB-OCT, compared with only 3.3% in TW^- group ($p<0.05$). 34 patients in the TW^+ group demonstrated marked dilatation of medium-sized and small airways. Higher baseline neutrophil elastase activity and TW^+ bronchioles on CT predicted progression of bronchiectasis.

Conclusion Thickened-walled bronchioles surrounding the dilated bronchi, identified with EB-OCT, indicates progression of bronchiectasis.

Introduction

Bronchiectasis is pathologically defined as the irreversible dilation of the tracheobronchial tree. Because chronic airway infections, inflammation and destruction are the core elements driving the progression of bronchiectasis [1], breaking this vicious cycle is central to the treatment of bronchiectasis. Early identification and diagnosis may help improve the management of bronchiectasis [2, 3].

However, few studies have revealed the mechanisms of pathogenesis, especially how bronchiectasis initially develops [4, 5]. Chest high-resolution computed tomography (HRCT) images have revealed that

the bronchioles with thickened walls surrounding the dilated bronchi might progress into typical radiological bronchiectasis [6, 7]. However, without the use of sophisticated and quantitative analytic software, which has not been adopted extensively for clinical application, chest HRCT might be capable of evaluating the airways up to the sixth-generation bronchi. Direct airway morphological assessment may help to probe the early morphological changes (bronchial dilatation and remodelling) with a greater resolution. The advent of endobronchial optical coherence tomography (EB-OCT) [8–10] has made it possible to evaluate the structural changes (including airway wall thickening) up to the ninth generation of bronchi in a real-time fashion.

We performed a longitudinal study with EB-OCT and chest CT to determine their diagnostic value for evaluating radiological progression of bronchiectasis by stratifying patients according to the presence/absence of tree-in-bud signs (the frequent chest imaging characteristics indicative of bronchial wall thickening) surrounding the dilated bronchi on chest HRCT images to the typical radiological bronchiectasis, and to explore the risk factors. Our findings may provide the rationale for early intervention of bronchial dilatation with inflammatory infiltration to prevent the progression to clinically significant bronchiectasis.

Methods

Study population

Between July 2014 and February 2017, we recruited consecutive patients with symptomatic bronchiectasis (part of the Progressive Bronchiectasis Early Surveillance Programme) from the Guangzhou Institute of Respiratory Diseases (Guangzhou, China). Eligible patients had radiological evidence of bronchiectasis, as evaluated centrally using chest HRCT by an experienced radiologist [11]. Patients were dichotomised into two groups based on the presence or absence of radiologist-reported tree-in-bud signs on baseline HRCT: those with tree-in-bud signs surrounding dilated bronchi (TW^+ group), and those without tree-in-bud signs surrounding dilated bronchi (TW^- group). All patients underwent OCT, HRCT, spirometry and sputum induction on the same day at baseline and 5-year longitudinal follow-up (no interim reassessments were performed). At longitudinal follow-up, the radiological progression of bronchiectasis was ascertained *via* both EB-OCT and HRCT.

The disease control group consisted of nine patients who underwent bronchoscopy for biopsy of lung nodules within the study time frame. Patients in the disease control group underwent a single chest HRCT and EB-OCT assessment at the initial visit only (no follow-up visits).

The study was approved by the ethics committee of the First Affiliated Hospital of Guangzhou Medical University (medical ethics approval 2014, no. 51), and all patients provided written informed consent.

Chest HRCT, spirometry and bronchiectasis severity index assessment

Unenhanced chest CT examinations were performed using different commercial CT scanners at baseline (Aquilion 16; Toshiba, Japan) and follow-up visits (Perspective 64; Siemens, Germany). Images were acquired during breath-hold at full inspiration. The fixed tube voltage was 120 kVp with adaptive current modulation. The raw imaging data were reconstructed into 2-mm slice thickness with the soft-tissue algorithm at baseline and 1-mm slice thickness at follow-up. The three-dimensional bronchial tree images were reconstructed using the DirectPath navigation system (version 1.1; Olympus, Japan). Bronchiectasis was diagnosed in cases where the internal diameter of bronchi greater than that of the accompanying pulmonary artery; there was a lack of normal bronchial tapering; or there were visible bronchi within 10 mm of the pleural surface. "Tree-in-bud sign" referred to centrilobular bronchial dilatation filled with mucus, pus or fluid [7]. The radiological severity of bronchiectasis was scaled by using a modified Reiff score on a lobar basis, where the lingular lobe was regarded as a separate lobe [12]. The maximal total score was 18 for six lobes [13]. Radiological progression of bronchiectasis was defined as the evolution from the initial tree-in-bud sign or thickened bronchial walls into the typical signs of bronchiectasis. Two chest radiologists (with 16 and 23 years' experience) independently scored the chest CT images. Progression of bronchiectasis could be ascertained only when the two radiologists reached a consensus.

Spirometry was conducted by using spirometers (QUARK PFT; COSMED, Milan, Italy), complying with the American Thoracic Society/European Respiratory Society guidelines [14]. Variation between the best two manoeuvres was <5% or 200 mL in forced vital capacity and forced expiratory volume in 1 s (FEV_1), with the maximal values being reported. The predicted values were calculated according to the model proposed by Zheng and Zhong [15].

The bronchiectasis severity index (BSI) [16] was adopted to rate the severity of bronchiectasis. The BSI comprises age, body mass index (BMI), prior exacerbations and prior hospitalisation in the preceding year,

FEV_1 % predicted, Medical Research Council dyspnoea score, the number of bronchiectatic lobes, *Pseudomonas aeruginosa* infection and colonisation with other potentially pathogenic micro-organisms. BSI of ⩽4, 5–8 and ⩾9 denoted mild, moderate and severe bronchiectasis, respectively.

Navigation planning, EB-OCT data acquisition and analysis

To more accurately evaluate airway structural changes (particularly the small airways), we performed EB-OCT assessment of the third- to ninth-generation bronchi surrounding the radiologically dilated bronchi. For patients in the TW^+ group, we initially labelled for EB-OCT measurement with the DirectPath version 1.1 navigation system, and advanced the detector to the bronchi with thickened walls or tree-in-bud sign surrounding the radiologically dilated bronchi on chest HRCT images. Typically, we selected three to five regions of interest (ROIs) where there were tree-in-bud signs within the diameter of 2 cm of the dilated bronchi on chest CT. The entry of these ROIs into the CT navigation system would allow us to establish a pathway which stemmed from the large airways to the tree-in-bud signs (bronchioles). We selected the ROIs within the diameter of 2 cm of the dilated bronchi on CT images because most of these affected bronchioles have already been located in the ninth-generation bronchi (the detection limit of EB-OCT) or more distal bronchioles. Only the ninth generation of the right lung bronchus 9 segment was subject to EB-OCT assessment among disease controls. In our study, ∼87% of patients in the TW^- group were subject to the measurement of the airway calibre at the same lung lobe as compared with those in the TW^+ group. The ninth-generation bronchi of the right lower lobe were evaluated as the control airway segment in a minority of patients who did not have bronchiectasis in the same lung lobe.

The bronchoscope with an EB-OCT detector was advanced into the target lobe with the Lightlabs C7XR OCT system (St Jude Medical, USA). The probe's outer diameter was 0.9 mm (C7 Dragonfly catheters), which could automatically rotate and pull back. We inserted the scanning probe with an ultrafine flexible bronchoscope (B260f; Olympus; outer diameter 2.8 mm, internal diameter 1.2 mm) to the labelled target bronchus, according to the planned pathway generated by the DirectPath system. Patients held their breath after full inspiration. The EB-OCT catheter was pulled back to the third-generation bronchus for automatic scanning. The identical virtual path was established for each patient to guide the EB-OCT detector to advance to an identical anatomical location. The EB-OCT scan was performed at a rotary frame rate of 180 Hz and a pullback rate of 1.8 $cm \cdot s^{-1}$, and hence 540 consecutive EB-OCT images were generated in each pullback procedure (length 5.4 cm) within 3 s. EB-OCT parameters included the mean luminal diameter (D_{mean}), inner airway area (A_i) and airway wall area (A_w) from the third to ninth generation. The airway wall area percentage (A_w%) was calculated as $(A_w/(A_i+A_w))\times100\%$ [17]. The EB-OCT parameters detected from the third to the fourth, from the fifth to the sixth, and from the seventh to the ninth generation of bronchi were averaged, respectively, to reflect the morphology of the large, medium-sized and small airways. Data were analysed using a computerised software (OCT system software; St Jude Medical). The normal range of the airway calibre has been published previously [8].

Sputum induction

Fresh induced sputum was sampled *via* induction with hypertonic saline (3–5%) during hospital visits. Following the removal of the content of the oral cavity and chest physical therapy for 15 min, patients expectorated into a 60-mL sterile clear plastic container. Eligible samples had ⩾25 leukocytes and ⩽10 epithelial cells under a microscopic field (×100). Within 2 h, sputum was split for bacterial culture and ultracentrifugation (50 000×*g*) at 4°C for 90 min to prepare sputum sol stored in −80°C freezers until further measurements.

Sputum bacterial culture

The methods for sputum bacterial culture have been described previously [13]. Briefly, fresh sputum was homogenised, followed by inoculation for overnight culture. Potentially pathogenic micro-organisms consisted of *P. aeruginosa*, *Haemophilus influenzae*, *Haemophilus parainfluenzae* and miscellaneous clinically significant bacteria [18]. Bacterial load, expressed as $CFU \cdot mL^{-1}$, was reported for the potentially pathogenic micro-organisms only.

Sputum biomarker assessments

Sputum matrix metalloproteinase (MMP)-9 level was measured using Luminex multiplex assay (Bio-Rad, USA) [13] with the Bio-Plex Reader (Bio-Rad). The lower and upper bounds of detection were 0.14 and 302.50 $ng \cdot mL^{-1}$, respectively, for MMP-9. Free neutrophil elastase (NE) activity was quantified in sputum supernatant using an NE activity assay kit according to the manufacturer's instructions (Cayman Chemicals, USA). Measurements were performed in duplicate and the mean was included for further analysis.

Statistical analysis

No formal sample size calculation could be made due to the lack of existing morphological data. We empirically aimed to recruit >50 patients each in the TW^+ and TW^- groups. Currently, the gold standard for defining the upper limit of the normal absolute internal diameter of bronchi is lacking. We defined bronchiectasis according to EB-OCT, provided that the airway internal diameter measured with EB-OCT at baseline was two times greater than that of the same corresponding bronchial segment among the age-matched healthy controls [8].

For the between-group comparisons, numerical data were presented as mean±SD for normal distribution or median (interquartile range) otherwise, and were compared using the two-sample independent t-test or Wilcoxon rank-sum test. Categorical data were expressed as number (percentage) and compared using the Chi-squared test. Bonferroni correction was applied to adjust for multiple comparisons. Correlation analyses were conducted using Pearson's or Spearman's model, with or without adjustment for confounding factors (age, sex, BMI). We calculated the difference of EB-OCT parameters by subtracting the values of the 5-year reassessment with those of the baseline levels.

A univariable logistic regression model was used to determine the associations between the radiological progression of bronchiectasis on EB-OCT and the clinical variables, including age, female sex, BMI, smoking status, duration of disease, respiratory symptoms at baseline, modified Reiff score, BSI, exacerbations within the previous 2 years, FEV_1 % pred, TW^+, sputum NE activity and MMP-9 levels at baseline, sputum bacterial density at baseline and the detection of *P. aeruginosa* at baseline. We only included parameters with both statistical ($p \leqslant 0.10$) and clinical significance into the multivariable logistic regression model: the BSI, exacerbations within the previous 2 years, FEV_1 % pred, TW^+, sputum NE activity and MMP-9 levels at baseline, and the detection of *P. aeruginosa* at baseline.

Statistical analysis was performed using SPSS (version 16.0; SPSS, USA) and GraphPad Prism 5.0 (GraphPad, USA). $p<0.05$ was deemed statistically significant for all analyses, unless otherwise stated.

Neither patients nor the public were involved in the design, conduct, reporting or dissemination of plans of our research.

Results

Patient characteristics

Out of 137 patients with bronchiectasis who underwent screening at baseline, 69 with tree-in-bud signs surrounding the dilated bronchi (TW^+) and 68 patients without tree-in-bud signs surrounding the dilated bronchi (TW^-) were included. 62 patients were excluded due to a variety of reasons (*e.g.* consent withdrawal or loss to follow-up); 75 patients and nine disease controls were included in the final analysis (figure 1).

Table 1 presents the baseline demographics and clinical characteristics. BSI was comparable between the TW^+ and TW^- groups ($p>0.05$). A higher proportion of patients in the TW^+ group had post-infectious bronchiectasis and isolation of *P. aeruginosa* than in the TW^- group (both $p<0.05$). Compared with the TW^- group, the TW^+ group had a lower BMI and more severe airflow limitation (both $p<0.05$). Most patients (98.4% in the TW^+ group and 96.7% in the TW^- group) had used mucolytics within the past 6 months, followed by theophylline (73.4% in the TW^+ group and 68.9% in the TW^- group).

Bronchiectasis detected with EB-OCT and HRCT measurement at the baseline visit

For the seventh to ninth generation of bronchi at baseline, the baseline EB-OCT metrics D_{mean} (mean 3.96 *versus* 2.05 mm, p=0.017), A_i (mean 10.25 *versus* 4.27 mm^2, p=0.005), A_w (mean 2.61 *versus* 0.83 mm^2, p=0.009) and A_w% (mean 19.64% *versus* 17.85%, p=0.039) of the bronchioles with thickened walls surrounding the dilated bronchioles (TW^+) on CT images were significantly greater than those of the same bronchiole segments in the TW^- group. However, at the third to sixth generation of bronchi, there were no significant differences in the D_{mean}, A_i and A_w between the TW^+ and TW^- groups at baseline visit (all $p>0.05$) (table 2). The tree-in-bud signs were mainly located in the lower lobes (67.2%), followed by the middle (including the lingula) lobe (28.1%).

Progression of bronchiectasis detected with EB-OCT and HRCT measurement

For the fifth- to sixth-generation bronchi, there was a significant increase from baseline in D_{mean} (mean difference 2.17, 95% CI 1.04–4.29), A_i (mean difference 14.39, 95% CI 8.63–21.64) and A_w (mean difference 2.68, 95% CI 2.12–3.06) and a decrease in A_w% (mean difference −3.1, 95% CI −5.21– −1.37) at 5-year follow-up in the TW^+ group, but not in the TW^- group. For the seventh- to ninth-generation bronchi, we also noted a significant increase from baseline in the D_{mean} (mean difference 1.97, 95% CI

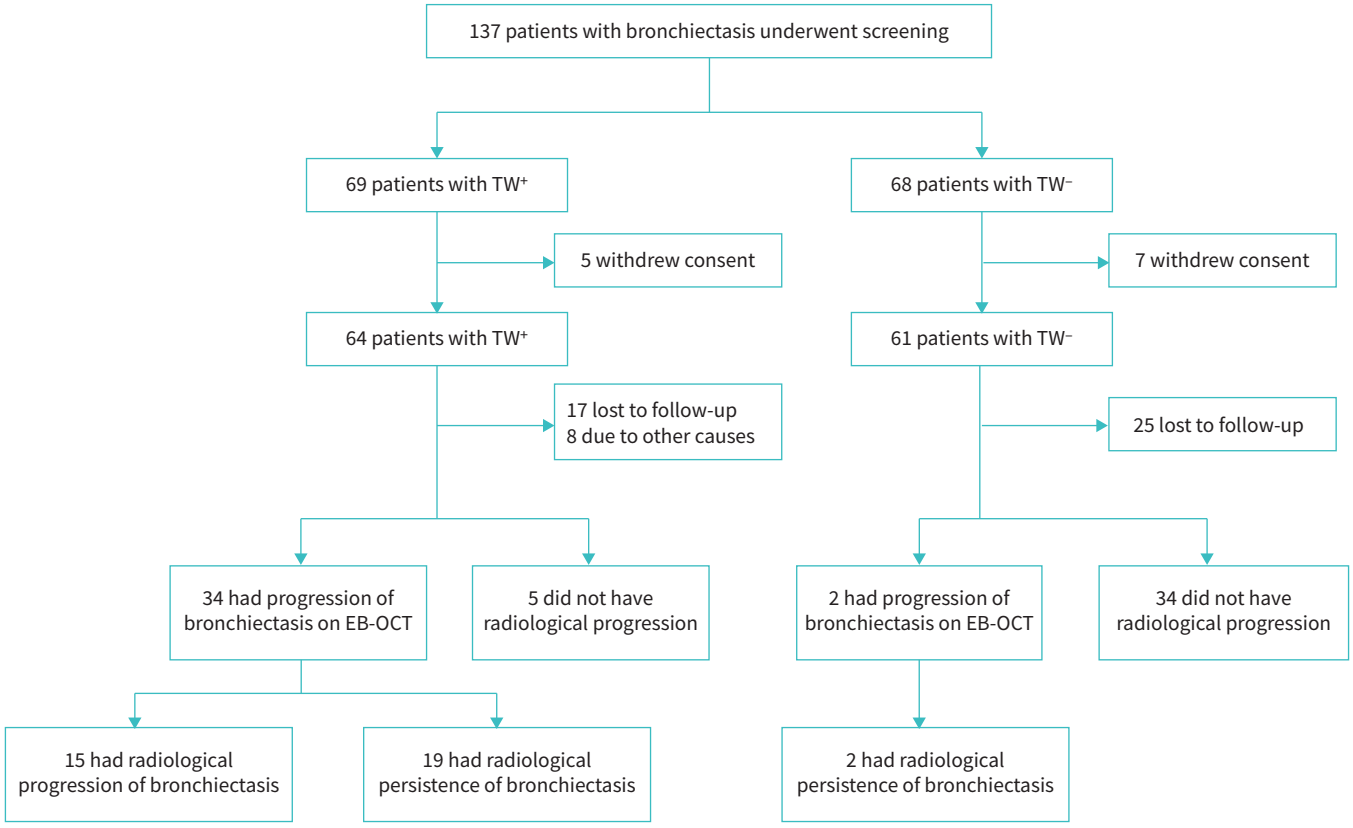

FIGURE 1 Subject recruitment flowchart. TW^+: bronchioles with thickened walls around dilated bronchioles (tree-in-bud sign) on computed tomography (CT) image; TW^-: bronchioles without thickened walls around dilated bronchioles (tree-in-bud sign) on CT image; EB-OCT: endobronchial optical coherence tomography.

1.59–2.75), A_i (mean difference 17.66, 95% CI 9.54–21.84) and A_w (mean difference 2.67, 95% CI 1.48–3.94) and a decrease in the A_w% (mean difference −3.27, 95% CI −6.16– −1.72) at 5-year follow-up in the TW^+ group, but not in the TW^- group (table 2).

At 5-year follow-up, the proportion of patients with an increase from baseline in the magnitude of bronchiectasis, measured with EB-OCT, was markedly higher in the TW^+ group than in the TW^- group (53.1% *versus* 3.3%, $p<0.05$). Of the 64 patients in the TW^+ group, 15 had developed typical bronchiectasis (11 cases in the lower lobes, eight cases in the middle lobe and four cases in both the middle and lower lobes). Meanwhile, the magnitude of bronchiectasis in HRCT scan was greater in the TW^+ group than in the TW^- group (23.4% *versus* 0%, $p<0.05$) as compared with baseline (figure 1). Furthermore, the bronchioles with radiologically visible thickened walls on the initial CT scans developed into the typical columnar or cystic bronchiectasis on HRCT at 5 years (figure 2).

Longitudinal EB-OCT measurement of the bronchioles

To confirm the structural changes of bronchioles on HRCT images obtained with EB-OCT, we next labelled the seventh to ninth generation of bronchi surrounding the dilated bronchi in the navigation system, which corresponded to the tree-in-bud signs of the same segment shown on chest HRCT (figure 3). In addition, we compared the changes during longitudinal follow-up with EB-OCT measurement. Figure 4 demonstrates the representative cross-sectional EB-OCT images of the third, fifth, seventh and ninth generation of bronchi in a 52-year-old female patient in the TW^+ group at baseline and at 5 years, and in a 46-year-old male patient with lung cancer (in the TW^- group) at baseline.

At 5 years, 34 (53.1%) out of 64 bronchiectasis patients in the TW^+ group demonstrated a marked dilatation of both the medium-sized (from the fifth to sixth generation) and small airways (from the seventh to ninth generation). However, no marked dilatation was observed corresponding to the third- and fourth-generation bronchi at 5 years. There was a notable increase in the $D_{5–6}$ (mean 3.90 *versus* 6.07 mm, $p<0.05$),

TABLE 1 Baseline levels of the bronchiectasis patients

	TW^+	TW^-	p-value
Patients	64	61	
Anthropometry			
Age, years	53.6±16.6	54.8±17.0	0.684
BMI, $kg \cdot m^{-2}$	19.34±2.21	20.29±3.44	0.039
Female	39 (60.9)	31 (50.8)	0.258
Nonsmoker	51 (79.7)	49 (80.3)	0.929
Disease-related parameters			
Disease duration, years	3.5 (2.3–4.9)	3.3 (2.1–4.8)	0.810
Acute exacerbations within 2 years	2 (1–2)	2 (1–2)	0.213
Bronchiectasis severity index	3 (2–4)	2 (2–3)	0.06
Imaging characteristics			
Bronchiectatic lobes	3 (2–3)	2 (2–3)	0.153
Modified Reiff score for HRCT	3.5 (3–4)	3 (2–4)	0.032
Lung segments with tree-in-bud signs	1 (1–2)	0 (0–0)	0.00
Location of tree-in-bud sign			
Upper lobe	3 (4.7)	0	0.260
Middle lobe and lingula	18 (28.1)	0	<0.001
Lower lobe	43 (67.2)	0	<0.001
Lung function indices			
FEV_1, % predicted	54.3±15.8	62±19.6	0.018
FVC, % predicted	68.3±11.3	78.1±19.2	0.001
FEV_1/FVC, %	68.4±14.4	70.7±14.1	0.359
D_{LCO}, % predicted	74.3±19.4	86.4±17.4	<0.001
Aetiology			
Post-infectious	24 (37.5)	13 (21.3)	0.047
Immunodeficiency	9 (14.1)	7 (11.5)	0.665
Miscellaneous	5 (7.8)	8 (13.1)	0.332
Idiopathic	26 (40.6)	33 (54.1)	0.131
Sputum bacteriology			
Pseudomonas aeruginosa	48 (75)	6 (9.8)	<0.001
Haemophilus influenzae	6 (9.4)	17 (27.9)	0.008
Other potentially pathogenic bacteria	1 (1.6)	11 (18)	0.002
Commensals	1 (1.6)	13 (21.3)	<0.001
Medication ever used within past 6 months			
Inhaled corticosteroids	7 (10.9)	6 (9.8)	0.840
Mucolytics	63 (98.4)	59 (96.7)	0.531
Theophylline	47 (73.4)	42 (68.9)	0.571
Macrolides	23 (35.9)	26 (42.6)	0.444

Data are presented as n, mean±SD, n (%) or median (interquartile range), unless otherwise stated. TW^+: bronchioles with thickened walls around dilated bronchioles (tree-in-bud sign) on computed tomography (CT) image; TW^-: bronchioles without thickened walls around dilated bronchioles (tree-in-bud sign) on CT image; BMI: body mass index; HRCT: high-resolution computed tomography; FEV_1: forced expiratory volume in 1 s; FVC: forced vital capacity; D_{LCO}: diffusing capacity of the lung for carbon monoxide.

$A_{i5–6}$ (mean 13.76 *versus* 28.15 mm^2, p<0.05), $D_{7–9}$ (mean 3.96 *versus* 5.93 mm, p<0.05) and $A_{i7–9}$ (mean 10.25 *versus* 27.91 mm^2, p<0.05) at 5 years as compared with the baseline levels (table 2). At 5 years, there were no significant changes in the EB-OCT metrics of all airway segments (large-to-medium plus small airways) in the TW^- group ($D_{3–4}$ mean 5.21 *versus* 4.88 mm, p>0.05; $A_{i3–4}$ mean 24.61 *versus* 21.75 mm^2, p>0.05; $D_{5–6}$ mean 3.84 *versus* 4.20 mm, p>0.05; $A_{i5–6}$ mean 17.18 *versus* 19.50 mm^2, p>0.05; $D_{7–9}$ mean 2.05 *versus* 2.28 mm, p>0.05; and $A_{i7–9}$ mean 4.27 *versus* 4.64 mm^2, p>0.05) compared with baseline levels. According to the assessment made by two independent radiologists, there were no significant changes in the airway diameter (progression to radiologically typical bronchiectasis) on chest HRCT in the TW^- group.

Associations between the progression on EB-OCT assessment and clinical characteristics of bronchiectasis

The associations between the progression of bronchiectasis measured with EB-OCT and the clinical characteristics (*e.g.* CT parameters, lung function, inflammatory markers and microbiology) are shown in table 3.

https://doi.org/10.1183/23120541.00490-2022

TABLE 2 Endobronchial optical coherence tomography (EB-OCT) parameters at baseline and at 5 years' follow-up

	Control	TW^+				TW^-				p-value[¶]	p-value[+]
		Baseline	5 years	Difference (95% CI)[#]	p-value	Baseline	5 years	Difference (95% CI)[#]	p-value		
Patients		64	39			61	36				
Large airways											
$D_{3–4}$, mm	5.60±1.08	5.05±1.96	5.23±2.09	0.18 (−0.21–1.16)	0.388	5.21±2.08	4.88±1.38	−0.33 (−1.13–0.48)	0.514	0.277	0.387
$A_{i3–4}$, mm^2	25.51±9.69	23.23±18.05	26.71±12.48	3.48 (−1.61–10.37)	0.074	24.61±17.97	21.75±9.69	−2.86 (−9.85–4.13)	0.652	0.739	0.152
$A_{w3–4}$, mm^2	3.33±0.97	3.71±0.91	3.41±1.46	−0.30 (−0.94–0.11)	0.539	2.79±1.00	3.52±1.32	0.73 (0.17–1.28)	0.148	0.085	0.528
Medium-sized airways											
$D_{5–6}$, mm	3.76±1.26	3.90±1.03	6.07±2.39	2.17 (1.04–4.29)	0.011	3.84±0.90	4.20±1.10	0.49 (−0.03–1.02)	0.761	0.671	0.029
$A_{i5–6}$, mm^2	18.27±6.11	13.76±6.78	28.15±4.31	14.39 (8.63–21.64)	0.006	17.18±8.27	19.50±8.46	2.46 (−2.17–7.09)	0.079	0.084	0.008
$A_{w5–6}$, mm^2	2.05 ±0.31	1.96±0.29	4.64±0.82	2.68 (2.12–3.06)	0.015	1.95±0.28	2.27±0.39	0.35 (0.16–0.54)	0.236	0.373	0.013
$A_{w5–6}$, %	11.20 ±4.59	16.66±9.10	13.56±5.81	−3.1 (−5.21– −1.37)	0.042	13.79±12.47	12.10±5.36	−1.97 (−7.21–3.26)	0.442	0.086	0.041
Small airways											
$D_{7–9}$, mm	1.84±0.46	3.96±0.91	5.93±1.54	1.97 (1.59–2.75)	0.029	2.05±0.63	2.28±0.51	0.22 (−0.10–0.53)	0.752	0.017	0.002
$A_{i7–9}$, mm^2	3.32±1.66	10.25±4.62	27.91±4.73	17.66 (9.54–21.84)	0.004	4.27±2.05	4.64±2.38	0.43 (−0.81–1.67)	0.493	0.005	0.001
$A_{w7–9}$, mm^2	0.62±0.31	2.61±0.84	5.28±1.93	2.67 (1.48–3.94)	0.027	0.83±0.33	0.76±0.11	−0.11 (−0.24–0.03)	0.516	0.009	0.001
$A_{w7–9}$, %	16.70±5.25	19.64±7.38	16.37±3.87	−3.27 (−6.16– −1.72)	0.016	17.85±10.91	17.49±9.87	−1.14 (−6.89–4.62)	0.691	0.039	0.027

Data are presented as n or mean±SD, unless otherwise stated. TW^+: bronchioles with thickened walls around dilated bronchioles (tree-in-bud sign) on computed tomography (CT) image; TW^-: bronchioles without thickened walls around dilated bronchioles (tree-in-bud sign) on CT image; D: inner diameter; A_i: inner luminal area; A_w: airway wall area; 3–4: from third- to fourth-generation bronchi; 5–6: from fifth- to sixth-generation bronchi; 7–9: from seventh- to ninth-generation bronchi. [#]: 5-year reassessment values minus those of the baseline levels; [¶]: comparison of each of the EB-OCT parameter between the TW^+ and TW^- groups at baseline; [+]: comparison of each of the EB-OCT parameters between the TW^+ and TW^- groups at 5 years.

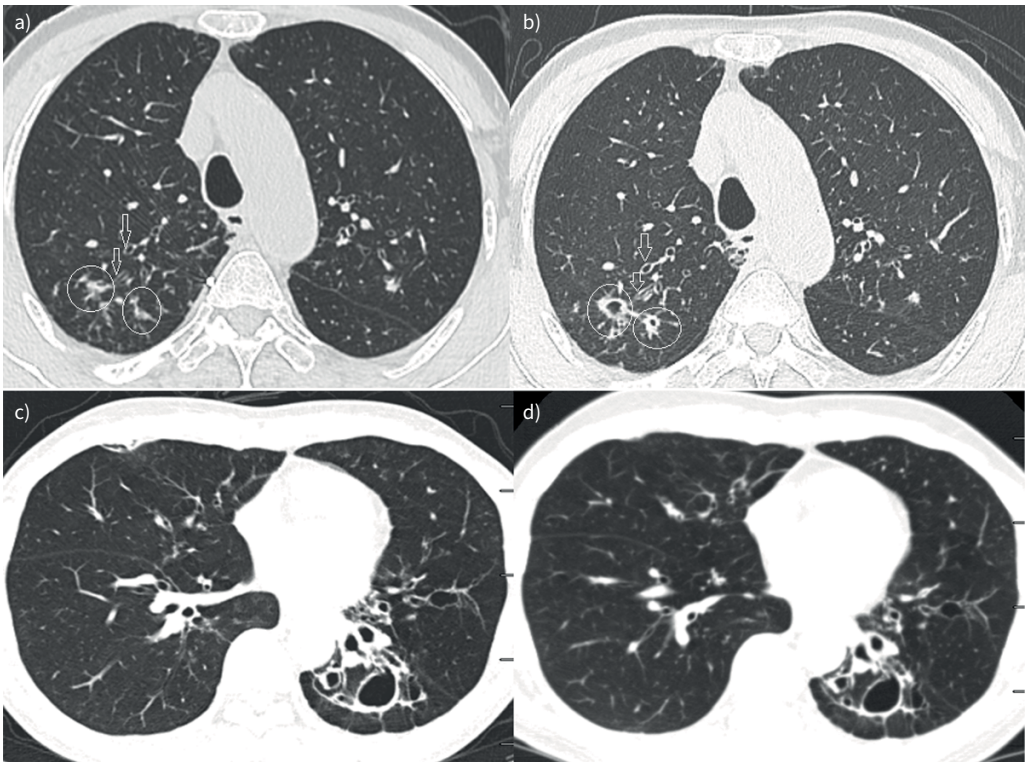

FIGURE 2 Longitudinal changes in chest radiological manifestations in a patient in the TW^+ group (presence of thickened-walled bronchioles surrounding dilated bronchi) and a patient in the TW^- group (absence of thickened-walled bronchioles surrounding dilated bronchi) during the 5-year follow-up. a, b) longitudinal changes in chest radiological manifestations in a 77-year-old male (TW^+ group); c, d) longitudinal changes in chest radiological manifestations in a 49-year-old male (TW^- group). a) The bronchioles surrounding the dilated bronchi are characterised by thickened walls or tree-in-bud signs, but no significant dilatation is shown on chest high-resolution computed tomographic scans at the initial visit; b) there are markedly dilated bronchioles at the same bronchial segment within the same patient after 5 years of follow-up. c, d) No tree-in-bud signs are developed after 5 years of follow-up in a patient who does not have tree-in-bud signs at the initial visit.

Multivariable logistic regression analysis was performed to determine the factors associated with the EB-OCT progression of bronchiectasis. Higher sputum NE activity (OR 1.05, 95% CI 1.01–1.10; p=0.030) and the TW^+ bronchioles on chest CT images (OR 140.42, 95% CI 1.03–19 077.11; p=0.048) were independently associated with the progression of bronchiectasis on EB-OCT.

Discussion

Progression of bronchiectasis has been attributed to the vicious cycle of chronic airway infection, inflammation and destruction [1]. Few studies have explored the morphological and radiological progression of bronchiectatic airways based on cohort study designs. How the unaffected bronchi progress to radiologically typical bronchiectasis remains unclear. In this study, we have demonstrated the longitudinal changes in the morphological characteristics of the dilated bronchi, evidenced by the thickened wall bronchioles surrounding the dilated bronchi visible on chest HRCT, or the tree-in-bud signs detected with EB-OCT. Our findings have provided higher-resolution images of different airway segments (particularly the small airways) in a real-time fashion. Apart from the higher sputum NE activity, the presence of bronchioles with thickened walls surrounding the dilated bronchi on HRCT at baseline could independently predict the progression of bronchiectasis at 5 years of follow-up.

Because of the limited resolution of chest HRCT, we have characterised the small airways using EB-OCT, which has been used to evaluate small airways in patients with COPD [17]. Identifying the events that predated the development of typical bronchiectasis may provide further clues to inform clinicians the key signs of radiological bronchiectasis progression. The vicious vortex hypothesis posits that both airway infection and inflammation (also indicated by the mucus plugging or infiltration) are imperative drivers of

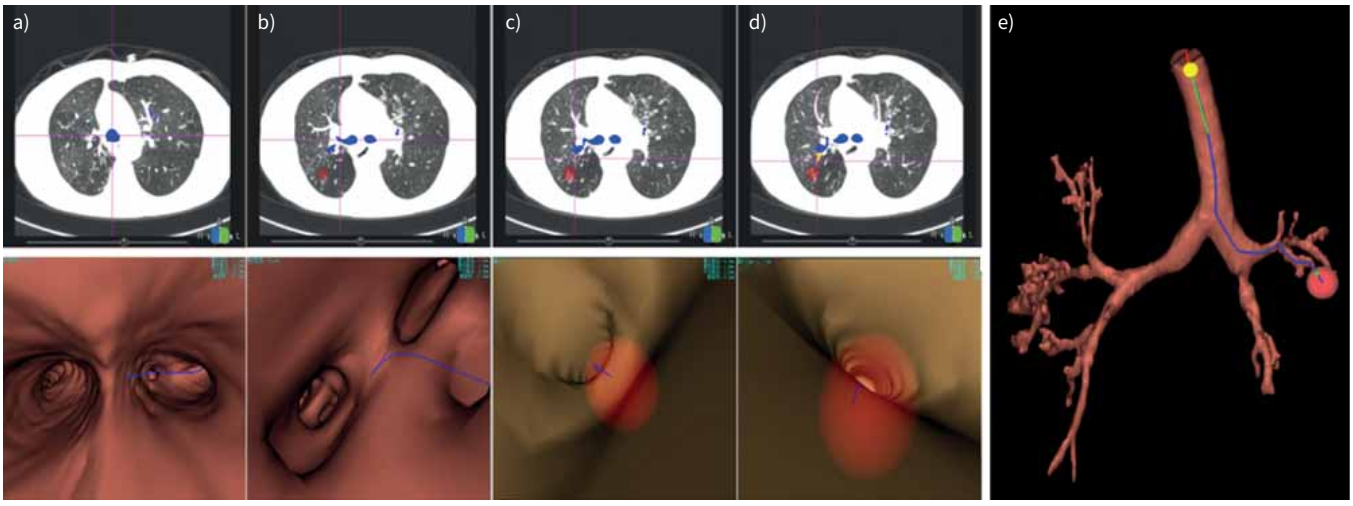

FIGURE 3 Chest high-resolution computed tomographic (HRCT) scans and visualisation with an automated navigation system. Chest HRCT images were obtained at 0.5–1.0 mm collimation in Digital Imaging and Communications in Medicine format, and transformed into the DirectPath version 1.1 navigation system (Olympus, Japan) for reconstruction of three-dimensional bronchial tree images. The bronchioles surrounding the dilated bronchi were labelled and the guided pathways were generated. The bronchoscope with detector was passed into the target bronchiole for endobronchial optical coherence tomography (EB-OCT) measurement according to the planned pathway generated by the DirectPath system. Cross-sectional and three-dimensional images of the a) carina, b) right main bronchus, c) right upper lobe bronchus and d) target bronchiole for the virtual path. e) The simulated guidance pathway (blue curve) to the target bronchiole (entry of the fibre bronchoscopy probe from the trachea to the target bronchiole).

bronchiectasis. To this end, we have specifically focused on the TW^{+} bronchi, which are mainly localised in the small airways. In our study, that the EB-OCT criteria detected more patients with radiological progression of bronchiectasis than the HRCT criteria could be partly interpreted by the greater ability of EB-OCT to directly evaluate the morphology of more distal airways. The difficulty in identifying the subtle structural changes in small airways could be circumvented with EB-OCT assessment. Here, we showed that the radiological bronchiectasis was more pronounced in small airways (mostly at the seventh- to ninth-generation bronchi) that had significant bronchial wall thickening and luminal dilatation, compared with the same bronchiolar segments from disease controls. However, neither the increased wall thickness of the proximal (third to fifth generation) bronchi nor the dilatation of the bronchial lumen was evident (figure 3, table 2). This might be because the distal bronchial wall thickness was less notable than that of the proximal bronchial wall, thus appearing more susceptible to the insult of the inflammatory responses or enzymatic digestion [19]. Due to the limited resolution, early-stage bronchial dilatation (particularly at the distal airways) could not be readily distinguished in the HRCT, apart from the tree-in-bud signs or bronchi with thickened walls [20].

Not all bronchi with tree-in-bud signs or thickened walls develop into typical radiological bronchiectasis. A previous study has reported that bronchiectasis is more prominent in the bronchioles surrounding the dilated bronchi [21]. Therefore, a lesion with dilatation of the bronchioles surrounding the radiologically typical dilated bronchi might be regarded as the characteristic sign of bronchiectasis. To verify this finding, we performed EB-OCT assessment on the bronchioles in patients with interstitial pneumonia and bronchiolitis obliterans with tree-in-bud signs or bronchiolitis on chest HRCT in our pilot study, with findings showing that these patients had thickening of the bronchial wall without bronchiectasis on both chest HRCT and EB-OCT images (Lin-ling Cheng *et al*., Guangzhou Medical University, Guangzhou, China; unpublished data). Therefore, the bronchioles with thickened walls surrounding the bronchi are susceptible to progression into the typical radiological dilatation. The diagnosis of these early signs of bronchiectasis could be based on the specific HRCT imaging characteristics (such as tree-in-bud signs or bronchi with thickened walls surrounding the dilated bronchi). EB-OCT might be valuable for detecting the early-stage bronchiectasis (figures 1 and 3). Our findings provide evidence that distal bronchiole dilation and higher sputum bacterial loads and higher concentrations of sputum MMP-8 and -9 might be predictors of the development of typical bronchiectasis on HRCT [22, 23]. In addition, our findings support the previous observation that higher NE activity is the key predictor of bronchiectasis development in children with cystic fibrosis [24].

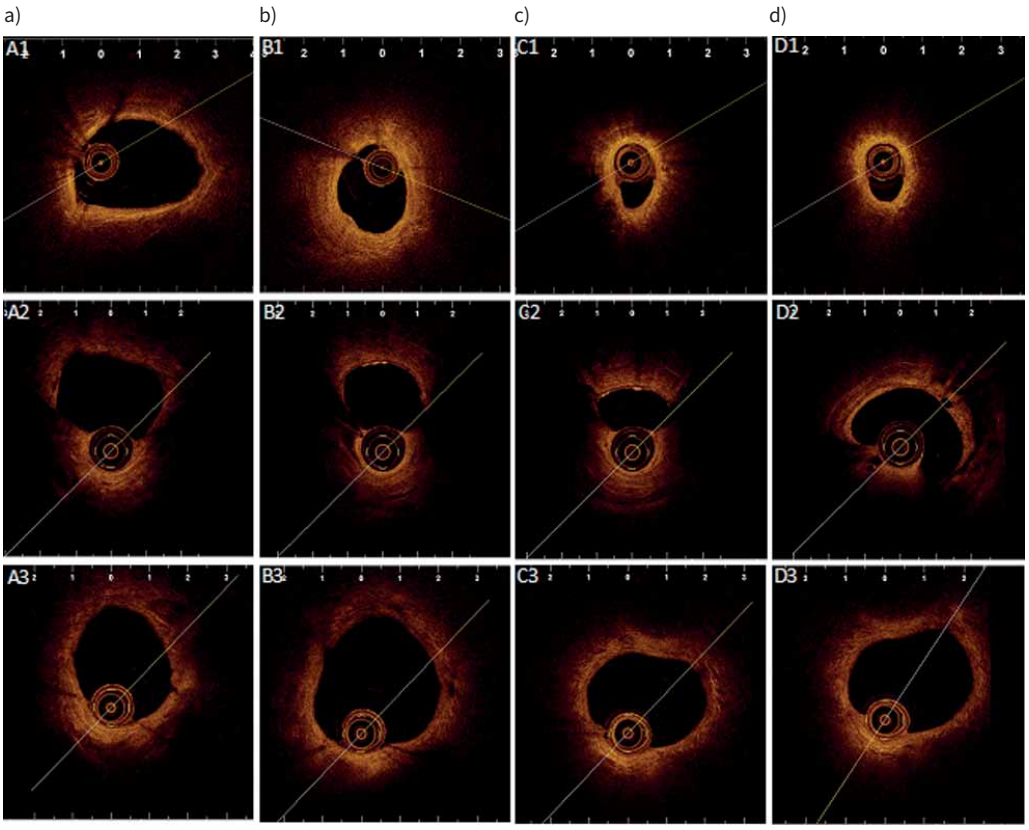

FIGURE 4 Cross-sectional endobronchial optical coherence tomography (EB-OCT) images of multiple airway generations in patients with (TW^+) and without (TW^-) tree-in-bud signs on computed tomography (CT). Cross-sectional images of EB-OCT in the a) third-, b) fifth-, c) seventh- and d) ninth-generation bronchi. A1, B1, C1 and D1 denote EB-OCT images of the third-, fifth-, seventh- and ninth-generation bronchi in the TW^- group. A2, B2, C2 and D2 denote the EB-OCT images of the third-, fifth-, seventh- and ninth-generation bronchi in the TW^+ group at baseline, and A3, B3, C3 and D3 denote the EB-OCT images of the third-, fifth-, seventh- and ninth-generation bronchi in the TW^+ group at 5 years. Compared with the images derived from the same bronchial segment of a representative patient in the TW^- group (C1, D1), the mean luminal diameter (D_{mean}), inner luminal area (A_i) and airway wall area (A_w) of the bronchioles with thickened walls surrounding the dilated bronchioles on CT images are significantly greater at the seventh to ninth generation of bronchi at the initial visit (C2, D2). Meanwhile, no differences could be found in the D_{mean}, A_i and A_w between the bronchioles at the third to fifth generation between a representative patient in the TW^+ group (A1, B1) and the TW^- group (A2, B2). At 5 years, there has been a marked dilatation of the fifth as well as from the seventh to ninth generation of bronchi (B3, C3, D3) as compared with the tree-in-bud signs at baseline (B2, C2, D2). No marked dilatation of the third-generation bronchi was noted (A3). The images at panels A2–D2 (at baseline) and A3–D3 (at 5-year longitudinal follow-up) were derived from the same bronchiectasis patient.

Progression to bronchiectasis has been observed in a subgroup of patients with cystic fibrosis [25]. In a study which recruited 168 patients with cystic fibrosis who had no detectable bronchiectasis on the first chest CT scan, 94 (56%) patients developed into radiologically typical bronchiectasis within a year [25]. Furthermore, air trapping on chest HRCT was associated with the subsequent development of typical bronchiectasis. Our findings indicated that progressive bronchial dilatation might have occurred in the bronchioles with thickened walls, which cannot be detected on the initial HRCT. The air trapping might be related to the thickening of the bronchial wall as well as mucus hypersecretion that results in mucus plugging and dynamic hyperinflation.

Notably, the bronchial dilatation surrounding the radiologically visible dilated bronchi independently predicted the development of typical bronchiectasis (table 3). Our findings have added to the vicious cycle theory that the progression of bronchiectasis could result from aggravated airway infections, heightened inflammatory responses and persistent airway destruction [26]. In line with our observations, Mott *et al.* [25]

https://doi.org/10.1183/23120541.00490-2022

TABLE 3 Clinical factors associated with progression of bronchiectasis

	Progression of bronchiectasis on EB-OCT		Univariable model		Multivariable model	
	No	Yes	OR (95% CI)	p-value	OR (95% CI)	p-value
Patients	39	36				
Age, years	56.5±16.7	50.4±17.6	0.98 (0.95–1.01)	0.124		
Female	19 (48.7)	23 (63.9)	0.54 (0.21–1.36)	0.188		
BMI, kg·m^{-2}	20.2±3.3	19.0±2.2	0.85 (0.72–1.01)	0.064		
Nonsmoker	32 (82.1)	27 (75)	1.52 (0.50–4.64)	0.458		
Duration of bronchiectasis, years	3.5 (2.2–5.6)	3.1 (2.3–4.7)	0.88 (0.69–1.11)	0.278		
Modified Reiff score for HRCT	3.0 (2.0–4.0)	4.0 (3.0–6.0)	1.68 (1.20–2.36)	0.003		
BSI	2.0 (2.0–3.0)	4.0 (3.0–4.3)	2.48 (1.52–4.04)	<0.001	2.08 (0.48–9.06)	0.330
Exacerbations within previous 2 years	1.0 (1.0–2.0)	2.0 (1.0–3.0)	1.79 (1.10–2.92)	0.020	1.10 (0.12–10.21)	0.935
FEV_1 % pred	61.0 (41.1–78.7)	54.3 (42.0–67.3)	0.98 (0.96–1.01)	0.148	1.01 (0.92–1.11)	0.850
Respiratory symptoms at initial visit	28 (71.8)	31 (86.1)	1.96 (0.64–6.02)	0.237		
Sputum NE activity at initial visit, µg·mL^{-1}	37.3 (22.6–70.9)	154.4 (123.8–173.4)	1.06 (1.03–1.10)	0.000	1.05 (1.01–1.10)	0.030
Sputum MMP-9 at initial visit, ng·mL^{-1}	353.3 (200.8–599.6)	1790.0 (1382.1–2509.0)	1.00 (1.00–1.01)	0.000	1.00 (1.00–1.00)	0.681
***P. aeruginosa* at initial visit**	2 (5.1)	31 (86.1)	5.13 (1.91–13.80)	0.001	4.18 (0.27–65.50)	0.308
Sputum bacterial densities at initial visit, ×10^7 CFU·mL^{-1}	6.4 (6.0–7.2)	7.1 (6.0–7.5)	1.06 (0.76–1.49)	0.724		
TW$^+$	5 (12.8)	34 (94.4)	115.60 (20.96–637.45)	<0.001	140.42 (1.03–19 077.11)	0.048
Inhaled corticosteroids	4 (10.3)	4 (11.1)				
Macrolides	17 (43.6)	10 (27.8)				
Mucolytics	39 (100)	36 (100)				
Theophylline	33 (84.6)	26 (72.2)				

Data are presented as n, mean±SD, n (%) or median (interquartile range), unless otherwise stated. The univariate logistic regression model was used to determine the associations between the radiological progression of bronchiectasis on endobronchial optical coherence tomography (EB-OCT) and the clinical variables, including age, female sex, body mass index (BMI), smoking status, duration of disease, respiratory symptoms at baseline, modified Reiff score, bronchiectasis severity index (BSI), exacerbations within the previous 2 years, forced expiratory volume in 1 s (FEV_1) % pred, bronchioles with thickened walls around dilated bronchioles (tree-in-bud sign) on computed tomography image (TW$^+$), sputum neutrophil elastase (NE) activity and matrix metalloproteinase (MMP)-9 levels at baseline, sputum bacterial density at baseline and the detection of *Pseudomonas aeruginosa* at baseline. We only included the parameters with both statistical ($p \leqslant 0.10$) and clinical significance in the multivariate logistic regression model: BSI, exacerbations within the previous 2 years, FEV_1 % pred, TW$^+$, sputum NE activity and MMP-9 levels at baseline and the detection of *P. aeruginosa* at baseline. HRCT: high-resolution computed tomography.

also found that the radiological progression of bronchiectasis was associated with heightened neutrophilic inflammation. Furthermore, the heightened elastase activity in sputum was associated with the BSI and radiological extent of bronchiectasis [27].

Some limitations should be taken into account. The detection of the more distal airways (*i.e.* the tenth generation and beyond) remains challenging, because the EB-OCT detector could not reach beyond the ninth generation, which has hampered the imaging of smaller or more distal bronchi surrounding the dilated bronchus shown on the chest CT. Moreover, because of the airway structural changes (*e.g.* alveolar or bronchiolar damage), the precise localisation of same the bronchioles before and after the 5-year longitudinal follow-up might not be feasible in some of the patients, despite the use of automated computerised software. Therefore, our data could not confirm whether the typical bronchiectasis evolved from the same dilated airway with early signs of bronchiectasis. Follow-up studies with a longer duration would enable a better longitudinal comparisons of the airway structural changes, thus providing greater insights into the patterns of bronchiectasis progression.

In summary, EB-OCT assessment reveals that the wall thickening of airways surrounding the dilated bronchi independently predicts progression to radiologically typical bronchiectasis. Our findings have further lent support to the vicious vortex hypothesis, suggesting the need for early detection and intervention of bronchiectasis to halt the vicious cycle.

Provenance: Submitted article, peer reviewed.

Author contributions: L-l. Cheng., W-j. Guan, C-h. Zhong, Z-q. Su, S-y. Li and N-s. Zhong were responsible for patient recruitment and collected individual data; C-y. Duan performed statistical analyses; L-l. Cheng, S-y. Li and N-s. Zhong contributed to study conception; L-l. Cheng and W-j. Guan drafted the manuscript; S-y. Li and N-s. Zhong provided critical review of the manuscript and approved the final submission.

Conflict of interest: W-j. Guan is an associate editor of this journal.

Support statement: This study was supported by National Natural Science Foundation grant 82170003 (to L-l. Cheng), The Study of the Common Key Technologies of Large-scale Development of Novel Inhaled Preparations grant 2017ZX09201002 (National Science and Technology Major Project of the Ministry of Science and Technology of China) (to N-s. Zhong), National Natural Science Foundation Outstanding Youth Fund grant N82222001, National Natural Science Foundation grant 81870003, Guangdong Science and Technology Foundation grant 2019B030316028, Zhongnanshan Medical Foundation of Guangdong Province grant ZNSA-2020013 and Guangzhou Science and Technology Plans grants 2023B03J0407 and 202102010372, and plan on enhancing scientific research in Guangzhou Medical University (to W-j. Guan). Funding information for this article has been deposited with the Crossref Funder Registry.

References

1 McShane PJ, Naureckas ET, Tino G, *et al.* Non-cystic fibrosis bronchiectasis. *Am J Respir Crit Care Med* 2013; 188: 647–656.
2 Barker AF. Bronchiectasis. *N Engl J Med* 2002; 346: 1383–1393.
3 Li AM, Sonnappa S, Lex C, *et al.* Non-CF bronchiectasis: does knowing the aetiology lead to changes in management? *Eur Respir J* 2005; 26: 8–14.
4 Tepper LA, Caudri D, Rovira AP, *et al.* The development of bronchiectasis on chest computed tomography in children with cystic fibrosis: can pre-stages be identified? *Eur Radiol* 2016; 26: 4563–4569.
5 Flume PA, Chalmers JD, Olivier KN. Advances in bronchiectasis: endotyping, genetics, microbiome, and disease heterogeneity. *Lancet* 2018; 392: 880–890.
6 Guan WJ, Gao YH, Xu G, *et al.* Characterization of lung function impairment in adults with bronchiectasis. *PLoS One* 2014; 9: e113373.
7 Gosset N, Bankier AA, Eisenberg RL. Tree-in-bud pattern. *AJR Am J Roentgenol* 2009; 193: W472–W477.
8 Su ZQ, Guan WJ, Li SY, *et al.* Evaluation of the normal airway morphology using optical coherence tomography. *Chest* 2019; 156: 915–925.
9 Hou R, Le T, Murgu SD, *et al.* Recent advances in optical coherence tomography for the diagnoses of lung disorders. *Expert Rev Respir Med* 2011; 5: 711–724.
10 Chen Y, Ding M, Guan WJ, *et al.* Validation of human small airway measurements using endobronchial optical coherence tomography. *Respir Med* 2015; 109: 1446–1453.
11 Feldman C. Bronchiectasis: new approaches to diagnosis and management. *Clin Chest Med* 2011; 32: 535–546.

12 Pasteur MC, Helliwell SM, Houghton SJ, *et al.* An investigation into causative factors in patients with bronchiectasis. *Am J Respir Crit Care Med* 2000; 162: 1277–1284.
13 Guan WJ, Gao YH, Xu G, *et al.* Sputum matrix metalloproteinase-8 and -9 and tissue inhibitor of metalloproteinase-1 in bronchiectasis: clinical correlates and prognostic implications. *Respirology* 2015; 20: 1073–1081.
14 Laszio G. Standardisation of spirometry. *Eur Respir J* 2005; 26: 319–338.
15 Zheng JP, Zhong NS. Normative values of pulmonary function testing in Chinese adults. *Chin Med J* 2002; 115: 50–54.
16 Chalmers JD, Goeminne P, Aliberti S, *et al.* The bronchiectasis severity index: an international derivation and validation study. *Am J Respir Crit Care Med* 2014; 189: 576–585.
17 Ding M, Chen Y, Guan WJ, *et al.* Measuring airway remodeling in patients with different COPD staging using endobronchial optical coherence tomography. *Chest* 2016; 150: 1281–1290.
18 Tunney MM, Einarsson GG, Wei L, *et al.* Lung microbiota and bacterial abundance in patients with bronchiectasis when clinically stable and during exacerbation. *Am J Respir Crit Care Med* 2013; 187: 1118–1126.
19 Marini T, Hobbs SK, Chaturvedi A, *et al.* Beyond bronchitis: a review of the congenital and acquired abnormalities of the bronchus. *Insights Imaging* 2017; 8: 141–153.
20 Hansell DM. Small airways diseases: detection and insights with computed tomography. *Eur Respir J* 2001; 17: 1294–1313.
21 Milliron B, Henry TS, Veeraraghavan S, *et al.* Bronchiectasis: mechanisms and imaging clues of associated common and uncommon diseases. *Radiographics* 2015; 35: 1011–1030.
22 Pasteur MC, Bilton D, Hill AT. British Thoracic Society guideline for non-CF bronchiectasis. *Thorax* 2010; 65: Suppl 1: i1–i58.
23 Wang D, Luo J, Du W, *et al.* A morphologic study of the airway structure abnormalities in patients with asthma by high-resolution computed tomography. *J Thorac Dis* 2016; 8: 2697–2708.
24 Sly PD, Gangell CL, Chen L, *et al.* Risk factors for bronchiectasis in children with cystic fibrosis. *N Engl J Med* 2013; 368: 1963–1970.
25 Mott LS, Park J, Murray CP, *et al.* Progression of early structural lung disease in young children with cystic fibrosis assessed using CT. *Thorax* 2012; 67: 509–516.
26 Guan WJ, Gao YH, Xu G, *et al.* Bronchodilator response in adults with bronchiectasis: correlation with clinical parameters and prognostic implications. *J Thorac Dis* 2016; 8: 14–23.
27 Chalmers JD, Moffitt KL, Suarez-Cuartin G, *et al.* Neutrophil elastase activity is associated with exacerbations and lung function decline in bronchiectasis. *Am J Respir Crit Care Med* 2017; 195: 1384–1393.